

One Proximate Kitaev Spin Liquid in the K - J - Γ Model on the Honeycomb Lattice

Jiucui Wang¹, B. Normand,² and Zheng-Xin Liu^{1,*}

¹*Department of Physics, Renmin University of China, Beijing 100872, China*

²*Neutrons and Muons Research Division, Paul Scherrer Institute, CH-5232 Villigen-PSI, Switzerland*



(Received 3 April 2019; published 5 November 2019)

In addition to the Kitaev (K) interaction, candidate Kitaev materials also possess Heisenberg (J) and off-diagonal symmetric (Γ) couplings. We investigate the quantum ($S = 1/2$) K - J - Γ model on the honeycomb lattice by a variational Monte Carlo method. In addition to the “generic” Kitaev spin liquid (KSL), we find that there is just one proximate KSL (PKSL) phase, while the rest of the phase diagram contains different magnetically ordered states. The PKSL is a gapless Z_2 state with 14 Majorana cones, which in contrast to the KSL has a gapless spin response. In a magnetic field applied normal to the honeycomb plane, it realizes two of Kitaev’s gapped chiral spin-liquid phases, of which one is non-Abelian with Chern number $\nu = 5$ and the other is Abelian with $\nu = 4$. These two phases could be distinguished by their thermal Hall conductance.

DOI: 10.1103/PhysRevLett.123.197201

The Kitaev model [1] of bond-dependent Ising-type spin interactions on the honeycomb lattice offers exactly soluble examples of both gapped and gapless quantum spin liquids (QSLs). The magnetically disordered ground states of different QSLs are the consequence of strong intrinsic quantum fluctuations and provide particularly clean realizations of different fundamental phenomena. The gapped Kitaev QSL has Z_2 Abelian topological order, while the quintessential “Kitaev spin liquid” (KSL) is the gapless state whose low-energy excitations form two Majorana cones, whereas its Z_2 flux excitations are gapped. In an applied magnetic field, the Majorana cones become gapped and the resulting state is a chiral spin liquid (CSL) with Ising-type non-Abelian anyonic excitations, which have potential application in fault-tolerant topological quantum computation.

Thus, the experimental realization of the Kitaev model has moved to the forefront of research in strongly correlated materials. While transition-metal compounds with strong spin-orbit coupling do realize Kitaev-type interactions [2,3], these “candidate Kitaev” materials typically possess in addition significant non-Kitaev interactions, which lead to Na_2IrO_3 [4,5] and $\alpha\text{-RuCl}_3$ [6–9] exhibiting magnetic order at low temperatures. Although $\text{H}_3\text{LiIr}_2\text{O}_6$ [10] is not ordered, it appears to show strong impurity and extrinsic disordering effects. At the same order in a strong-coupling treatment [11], the Kitaev (K) interaction is accompanied by Heisenberg (J) and off-diagonal symmetric (Γ) interactions, and thus the focus of the field has become the understanding of “proximate Kitaev” physics in this class of model, also under applied magnetic fields [12–15] and pressures [16].

In this Letter, we investigate the K - J - Γ extended Kitaev model by variational Monte Carlo (VMC) studies of a

spinon representation. Guided by the projective symmetry group (PSG), we obtain the global K - J - Γ phase diagram and show that it contains two distinct QSL phases among several classically ordered phases. One QSL, at small J and Γ , is the generic KSL. At larger Γ we find one proximate KSL (PKSL), a non-Kitaev QSL sharing the same PSG as the KSL but with 14 Majorana cones in the first Brillouin zone and gapless spin excitations. In an applied \hat{c} -axis field, all 14 cones are gapped and the PKSL hosts two exotic CSL phases, one with non-Abelian anyons and one with Abelian anyons. These results shed crucial new light on the parameter-space constraints and (induced) spin-liquid phases of candidate Kitaev materials.

In the candidate materials known to date, $K < 0$ is believed to be ferromagnetic [17–20], while J has been argued to have both signs and extended nature, but all studies of the Γ (and Γ') term(s) take $\Gamma > 0$ [21,22]. The role of Γ in a fully quantum model remains little studied [23], but from classical models Γ is thought to explain the strongly anisotropic field response of $\alpha\text{-RuCl}_3$ [8,21]. In general, it is not yet accepted that a $J = 0$ (i.e., K - Γ) model can support a magnetically ordered ground state [21], and it has been claimed on the basis of exact diagonalization of small systems [11,24] and infinite-size density-matrix renormalization-group studies of narrow cylinders [25] that multiple QSL phases may exist in the K - J - Γ model at small J .

The model we consider is

$$H = \sum_{\langle i,j \rangle \in \gamma} K S_i^\gamma S_j^\gamma + J \vec{S}_i \cdot \vec{S}_j + \Gamma (S_i^\alpha S_j^\beta + S_i^\beta S_j^\alpha), \quad (1)$$

where $\langle i, j \rangle$ denotes nearest-neighbor sites and γ both the bond type on the honeycomb lattice and the spin index.

Because of the spin-orbit coupling, the symmetry group of the model, $G = D_{3d} \times Z_2^T$ where $Z_2^T = \{E, T\}$ is time reversal, is finite, meaning its elements are discrete operations combining the space-time and spin degrees of freedom.

We find the ground state of the $S = 1/2$ K - J - Γ model by VMC calculations, which is a powerful method for the study of spin-liquid phases. We first introduce the fermionic slave-particle representation $S_i^m = \frac{1}{2} C_i^\dagger \sigma^m C_i$, where $C_i^\dagger = (c_{i\uparrow}^\dagger, c_{i\downarrow}^\dagger)$, $m \equiv x, y, z$, and σ^m are Pauli matrices. The particle-number constraint, $\hat{N}_i = c_{i\uparrow}^\dagger c_{i\uparrow} + c_{i\downarrow}^\dagger c_{i\downarrow} = 1$, should be imposed at every site to ensure that the size of the fermion Hilbert space is the same as that of the physical spin. This complex fermion representation is equivalent to the Majorana representation introduced by Kitaev [1]. It has a local $SU(2)$ symmetry that is independent of the $SU(2)$ spin-rotation operations and can be considered as a gauge structure [26], as discussed in Sec. S1A of the Supplemental Material (SM) [27]. The spin interactions in Eq. (1) are rewritten in terms of interacting fermionic operators and decoupled into a noninteracting mean-field Hamiltonian (Sec. S1B of the SM [27]), which for the most general spin-orbit-coupled spin liquid has the form

$$H_{\text{mf}} = \sum_{\langle i, j \rangle \in \gamma} \text{Tr}[U_{ji}^{(0)} \psi_i^\dagger \psi_j] + \text{Tr}[U_{ji}^{(1)} \psi_i^\dagger (iR_{\alpha\beta}^\gamma) \psi_j] \\ + \text{Tr}[U_{ji}^{(2)} \psi_i^\dagger \sigma^\gamma \psi_j] + \text{Tr}[U_{ji}^{(3)} \psi_i^\dagger \sigma^\gamma R_{\alpha\beta}^\gamma \psi_j], \quad (2)$$

where $\psi_i = (C_i \bar{C}_i)$, $\bar{C}_i = (c_{i\downarrow}^\dagger, -c_{i\uparrow}^\dagger)^T$, $R_{\alpha\beta}^\gamma = -i(\sigma^\alpha + \sigma^\beta)/\sqrt{2}$ is a rotation matrix, and the quantities $U_{ji}^{(m)}$, with γ specified by $\langle i, j \rangle$, are mean-field parameters.

In the states described by Eq. (2), the $SU(2)$ gauge symmetry is usually reduced to $U(1)$ or Z_2 , which is known as the invariant gauge group (IGG) [35]. The Majorana mean-field solution of the Kitaev model has IGG Z_2 . Because the KSL is a special (exactly soluble) point in the model of Eq. (1), one expects a finite regime of QSL states connected adiabatically to it; following Ref. [36] we call this the generic KSL (GKSL). A QSL ground state preserves the full symmetry group G and so does the mean-field Hamiltonian. However, a general symmetry operation of this Hamiltonian is a space-time and spin operation in G combined with an $SU(2)$ gauge transformation. These new symmetry operations form a larger group, known as the PSG, which is equivalent to a central extension of G by the IGG (Sec. S2 of the SM [27]). The PSG of the KSL is known exactly [37] and the corresponding mean-field Hamiltonian must respect it. The PSG reduces the number of independent parameters and, as detailed in Sec. S3 of the SM [27], the coefficients $U_{ji}^{(m)}$ in Eq. (2) are constrained to the forms $U_{ji}^{(0)} = i\eta_0 + i(\rho_a + \rho_c)$, $U_{ji}^{(1)} = i(\rho_a - \rho_c + \rho_d)(\tau^\alpha + \tau^\beta) + i\eta_3(\tau^x + \tau^y + \tau^z)$,

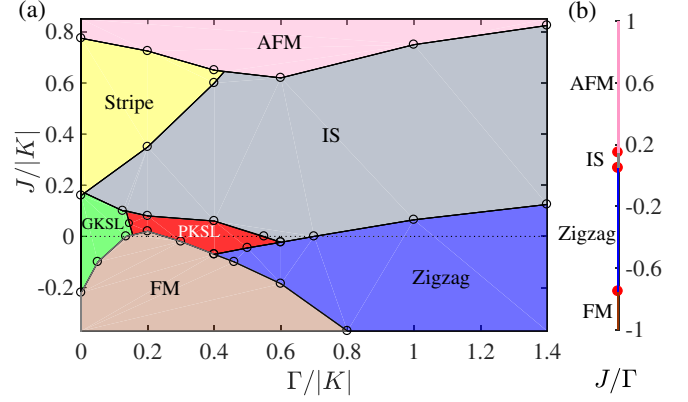


FIG. 1. (a) Phase diagram of the quantum K - J - Γ model for $K < 0$ in the limit of large system size. There are two QSL phases of different types but with the same PSG, the GKSL and the PKSL. The magnetically ordered phases are antiferromagnetic (AFM), stripe, incommensurate spiral (IS), zigzag, and ferromagnetic (FM) order. (b) Detail of the limit $|K|/\Gamma \rightarrow 0$, where all phases are magnetically ordered; the transitions occur at $J/\Gamma = 0.15, 0.05$, and -0.75 .

$$U_{ji}^{(2)} = i(\rho_a + \rho_c)\tau^\gamma + i\eta_5(\tau^x + \tau^y + \tau^z), \quad \text{and} \quad U_{ji}^{(3)} = i(\rho_c - \rho_a - \rho_d)(\tau^\alpha - \tau^\beta).$$

In addition, we allow competing magnetically ordered phases by including the term $H'_{\text{mf}} = \frac{1}{2} \sum_i \mathbf{M}_i \cdot C_i^\dagger \sigma C_i$ in the mean-field Hamiltonian [23]. The ordering pattern of \mathbf{M}_i is set from the classical solution within the single- \mathcal{Q} approximation, leaving only the amplitude M and the canting angle ϕ to be determined variationally (Sec. S3 of the SM [27]). The power of the VMC approach is that it allows the particle-number constraint to be enforced locally, by performing Gutzwiller projection of the mean-field ground states to obtain the trial wave functions $|\Psi(x)\rangle = P_G |\Psi_{\text{mf}}(x)\rangle$, where x denotes the variational parameters $(\rho_a, \rho_c, \rho_d, \eta_0, \eta_3, \eta_5, M, \phi)$. These are determined by minimizing the trial ground-state energy, $E(x) = \langle \Psi(x) | H | \Psi(x) \rangle / \langle \Psi(x) | \Psi(x) \rangle$, in calculations performed on tori of up to 14×14 unit cells, i.e., 392 lattice sites. Because the final variational states depend crucially on the mean-field Hamiltonian, a meaningful VMC procedure requires a careful choice and comparison of decoupling channels, and we have tested many spin-liquid and magnetic *Ansätze* (Sec. S3). Figure 1 shows the VMC phase diagram of the K - J - Γ model at zero applied field. As a benchmark, we note that our phase boundaries at $\Gamma = 0$, $J > 0$ agree quantitatively with those of Ref. [38]. Although the mean-field phase diagram contains a number of candidate QSLs, VMC calculations reveal that only two are robust. One is the GKSL, whose regime of stability is bounded approximately by $|J/K| = 0.2$ at $\Gamma = 0$ and $\Gamma/|K| = 0.15$; this result provides a quantitative statement of the region of relevance for the considerations of Ref. [36]. The second we name the PKSL, one of our central results being that there is only one QSL proximate

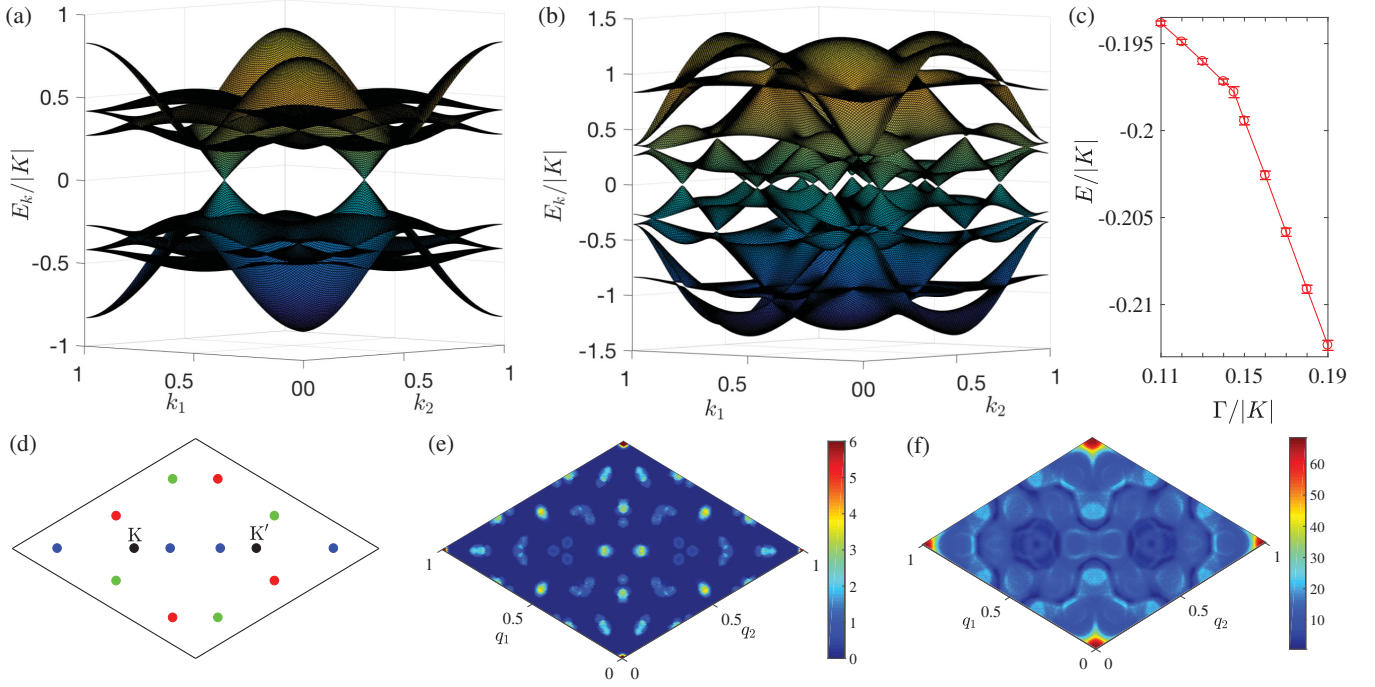


FIG. 2. (a) Spinon dispersion in the GKSL, drawn with $\Gamma/|K| = 0.1$ and $J = 0$, showing 2 Majorana cones. (b) Spinon dispersion in the PKSL, drawn with $\Gamma/|K| = 0.3$ and $J = 0$, showing 14 Majorana cones. (c) Ground-state energy per site of the K - J - Γ model at fixed $J/|K| = 0.05$, showing a clear first-order phase transition. (d) Locations of the 14 cones of the PKSL in the first Brillouin zone. (e) Dynamical structure factor of the PKSL at low energy (integrated over energies $0 \leq \omega/|K| \leq 0.08$). (f) Dynamical structure factor of the PKSL at $\omega/|K| = 0.15$ (integrated over $0.13 \leq \omega/|K| \leq 0.17$).

to the GKSL. The GKSL and PKSL have the same PSG despite being physically quite different states. In contrast to the spinon excitation spectrum of the GKSL, which has two Majorana cones in the first Brillouin zone [Fig. 2(a)], the PKSL has 14 [Figs. 2(b) and 2(d)]. These cones are protected from local perturbations by the combination of spatial-inversion and time-reversal symmetry, as detailed in Sec. S3 of the SM [27]. We discuss the nature of the cones and the magnetic response of the PKSL below.

The majority of the phase diagram (Fig. 1) consists of the magnetically ordered states familiar from the classical K - J - Γ model [11], namely AFM, stripe, incommensurate spiral (IS), zigzag, and FM ordered phases. Unsurprisingly, the boundaries around the QSL phases are rather different in the quantum model, with FM being stronger at low Γ and IS extending to $J < 0$. We comment that not only can an incommensurate ordered phase still exist for $S = 1/2$, but it can also exist throughout the phase diagram from (near) a pure K - Γ to a pure J - Γ model; as expected of our ordered phases, the spiral angles we obtain agree with Ref. [11]. We draw attention to the fact that all of the $J = 0$ line in Fig. 1 is ordered for $\Gamma/|K| > 0.55$, with IS order until $\Gamma/|K| = 0.7$ and zigzag order all the way to and in the pure Γ model [39]. This result contradicts an infinite-size density-matrix renormalization-group study of [25] that reported only QSL phases in the K - Γ model; as we show in Sec. S4 of the SM [27], that conclusion is relevant only for very narrow

cylinders. While the existence of order has been called into question at $J = 0$ [21], it is robust in the $S = 1/2$ model in VMC.

We state without demonstration that all of the phase transitions between the magnetically ordered phases are first-order, which is the simplest possibility when two phases of differing order parameters meet. A more complex situation is possible for the transitions between ordered and QSL phases, which could be second-order or even show an intermediate phase with coexisting magnetic and Z_2 topological order (Sec. S3 of the SM [27]). However, we find at all points we have investigated that these transitions are also first-order. Finally, the transition between the GKSL and PKSL is also sharply first-order, as may be observed both in the ground-state energy [Fig. 2(c)] and through discontinuities in the optimal variational parameters (not shown). Neither the GKSL nor the PKSL dispersion [Figs. 2(a) and 2(b)] evolves significantly around the level-crossing.

Returning to the spin response of the QSLs, it is helpful to consider Kitaev's representation [1] of the spin in terms of Majorana fermions, $S^m = ib^m c$ ($m = x, y, z$), which we review in Sec. S1 of the SM [27]. In the GKSL, the c fermions are gapless and the b^m fermions gapped, but the gapped spin response of the KSL becomes gapless when both J and Γ are nonzero [36]. This is verified in our VMC calculations in the form of c - b^m hybridization in the low-energy limit, but as shown in Sec. S5 of the SM [27]

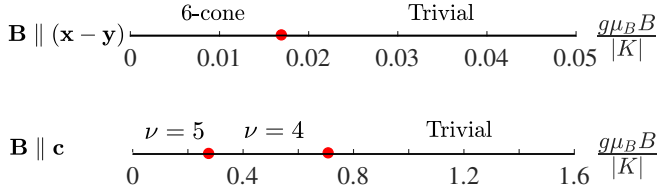


FIG. 3. Phase diagrams of the PKSL ($\Gamma/|K| = 0.3$, $J = 0$) in a magnetic field applied in the $\hat{x} - \hat{y}$ direction and in the $\hat{c} = (\hat{x} + \hat{y} + \hat{z})/\sqrt{3}$ direction. “6-cone” denotes a phase whose low-energy spinon dispersion has six remaining cones.

this hybridization remains very weak throughout the GKSL regime, such that low-energy spin excitations, if present, have very little weight. By contrast, in the PKSL we find that the quasiparticles are strongly hybridized combinations of c and b^m fermions at all wave vectors and energies, which is a consequence of the finite η_3 parameter induced by the Γ term. Thus, low-energy spin excitations arise from both intra- and intercone spinon processes and the spin response of the PKSL is gapless, as we illustrate in Fig. 2(e) by computing the dynamical structure factor $S(\mathbf{q}, \omega)$ at the mean-field level for energy $\omega = 0$ (Sec. S5). The positions of the maxima are readily understood from the cone structure shown in Fig. 2(d). For energies beyond the cone region, $S(\mathbf{q}, \omega)$ takes on a complex and continuous form [Fig. 2(f)].

One of the most exciting properties of the KSL is that it becomes a gapped, non-Abelian CSL in an applied magnetic field of any orientation not orthogonal to an Ising (spin) axis. Specifically, Kitaev classified 16 different types of CSL based on the statistics of their vortices, which are defects arising from inserted flux quanta [1]. He showed that these Z_2 vortices are Abelian anyons when the Chern number ν is even and non-Abelian anyons when ν is odd, leading to a clear illustration of topological properties, edge modes, fusion rules, and applications in quantum computation. The KSL in a field provides an example of the class $\nu = 1$, where the non-Abelian statistics arise due to unpaired Majorana modes (σ in Table I) associated with the vortices. By VMC calculations in a field $\mathbf{B} \parallel \hat{c}$ (Sec. S6 of the SM [27]), we verify at the mean-field level that these modes are also present in the GKSL; this non-Abelian regime is terminated at a Z_2 deconfinement-to-confinement transition [38].

In the PKSL, each of the seven pairs of cones becomes gapped in a field $\mathbf{B} \parallel \hat{c}$ and contributes a Chern number $\nu = \pm 1$. We demonstrate by VMC calculations at $\Gamma/|K| = 0.3$ and $J = 0$ that a CSL phase with $\nu = 5$ is obtained at small $|\mathbf{B}|$. As shown in Fig. 3, there are two successive, weakly first-order phase transitions with increasing $|\mathbf{B}|$, to a $\nu = 4$ CSL and then to a trivial phase connected to the fully polarized state. (We comment that this trivial, Z_2 -confined phase is obtained from both the $\nu = 1$ and $\nu = 0$ mean-field states, as shown in Sec. S6 of the SM [27].) Thus the PKSL

TABLE I. Field-induced CSL states realized to date in K - J - Γ models. ν is the Chern number. KL is the Kalmayer-Laughlin state [23,40]. 1 denotes the vacuum and ε the fermion. σ denotes the vortices in the non-Abelian phases ($\nu = 1$ and 5), which have topological spin $e^{i(\pi/8)}$ and $e^{i(5\pi/8)}$. e and m are the two different types of vortex in the Abelian CSL ($\nu = 4$), which are both semions. GSD abbreviates the ground-state degeneracy on a torus. c_- is the chiral central charge.

Parent state	CSL	Topological sectors	GSD	c_-
PKSL	$\nu = 5$	$\sigma, \varepsilon, 1$	3	5/2
PKSL	$\nu = 4$	$e, m, \varepsilon, 1$	4	2
KSL	$\nu = 1$	$\sigma, \varepsilon, 1$	3	1/2
U(1) Dirac	KL	$e, 1$	2	1

provides a specific realization of two little-known cases from Kitaev’s “16-fold way,” and we use it in Sec. S6 to illustrate their vortex modes at the mean-field level. The $\nu = 5$ phase is a non-Abelian CSL while the $\nu = 4$ phase is Abelian. Quite generally, in a CSL with Chern number ν , there are ν branches of chiral Majorana edge states, each of which contributes to a total chiral central charge $c_- = \nu/2$. The thermal Hall conductance, which is a physical observable, is therefore quantized to $\kappa_{xy}/T\Lambda = c_-$, where $\Lambda = \pi k_B^2/6h$ is a constant. From the number of associated midgap modes it can be shown that the vortex carries topological spin $e^{i\nu(\pi/8)}$, and from its fusion with itself or with a fermion we obtain the anyonic character of the CSLs as listed in Table I. These results are further verified within our VMC analysis by calculating the ground-state degeneracy (GSD) on a torus, which matches the number of topologically distinct quasiparticle types.

In contrast to the emergence in an arbitrary applied field of fully gapped quantum states, which can be distinguished by their ν or edge c_- numbers, is the possibility that, for specific field directions, the system remains a gapless Z_2 QSL over a finite range of field magnitudes [23]. In the PKSL we find this to be the case for $\mathbf{B} \parallel (\mathbf{x} - \mathbf{y})$, where the six black and blue cones shown in Fig. 2(d) remain gapless at low fields, whereas the other cones become gapped. For $\mathbf{B} \parallel (\mathbf{y} - \mathbf{z})$, the black and red cones remain gapless and for $\mathbf{B} \parallel (\mathbf{z} - \mathbf{x})$ the black and green cones. With increasing field, pairs of cones move towards each other, but a first-order transition occurs to a fully gapped state at a critical field $B_c \simeq 0.017|K|/g\mu_B$ (Fig. 3). This reflects the fact that many competing states appear at these low energy scales. We leave the response of the PKSL to fields of arbitrary orientation and strength to a future study.

The K - J - Γ model is expected to provide the basis for interpreting the physics of 4d and 5d transition-metal compounds. While robust magnetic order suggests strong J terms in Li_2IrO_3 and Na_2IrO_3 [4,5], α - RuCl_3 is thought to have only weak J [20] and many different K and Γ combinations have been suggested [21,22]. Our phase

diagram provides a quantitative guide to the low- J , low- Γ parameter regime required to observe QSL behavior, including by application of pressure to the known candidate materials. It also offers a detailed framework within which to interpret both the physics of the magnetically disordered material $\text{H}_3\text{LiIr}_2\text{O}_6$ [10] and the reported observation of a half-integer-quantized thermal Hall conductance in $\alpha\text{-RuCl}_3$ [41].

In summary, we have obtained the phase diagram of the quantum $K\text{-}J\text{-}\Gamma$ model on the honeycomb lattice. We find two quantum spin-liquid phases, the generic KSL and one proximate KSL, that have the same projective symmetry group but quite different low-energy physics. The PKSL is a gapless Z_2 QSL with 14 Majorana cones and a gapless spin response. In an applied field it realizes a gapped, non-Abelian chiral QSL with $\nu = 5$ and an Abelian one with $\nu = 4$. We also map the wide variety of magnetically ordered phases appearing in the quantum limit. Our phase diagram provides an essential guide to the physics of candidate Kitaev materials.

We thank M. Cheng, H.-J. Liao, Q. Luo, M. Vojta, C. Wang, T. Xiang, Q. Wang, and especially Y.-M. Lu and L. Zou for helpful discussions. This work was supported by the Ministry of Science and Technology of China (Grant No. 2016YFA0300504), the NSF of China (Grants No. 11574392 and No. 11974421), and the Fundamental Research Funds for the Central Universities and the Research Funds of Renmin University of China (No. 19XNGL11).

*liuzxphys@ruc.edu.cn

- [1] A. Kitaev, *Ann. Phys. (Amsterdam)* **321**, 2 (2006).
- [2] G. Jackeli and G. Khaliullin, *Phys. Rev. Lett.* **102**, 017205 (2009).
- [3] J. Chaloupka, G. Jackeli, and G. Khaliullin, *Phys. Rev. Lett.* **105**, 027204 (2010).
- [4] F. Ye, S. X. Chi, H. B. Cao, B. C. Chakoumakos, J. A. Fernandez-Baca, R. Custelcean, T. F. Qi, O. B. Korneta, and G. Cao, *Phys. Rev. B* **85**, 180403(R) (2012).
- [5] S. K. Choi, R. Coldea, A. N. Kolmogorov, T. Lancaster, I. I. Mazin, S. J. Blundell, P. G. Radaelli, Y. Singh, P. Gegenwart, K. R. Choi, S.-W. Cheong, P. J. Baker, C. Stock, and J. Taylor, *Phys. Rev. Lett.* **108**, 127204 (2012).
- [6] J. M. Fletcher, W. E. Gardner, A. C. Fox, and G. Topping, *J. Chem. Soc. A* 1038 (1967).
- [7] J. A. Sears, M. Songvilay, K. W. Plumb, J. P. Clancy, Y. Qiu, Y. Zhao, D. Parshall, and Y.-J. Kim, *Phys. Rev. B* **91**, 144420 (2015).
- [8] R. D. Johnson, S. C. Williams, A. A. Haghighirad, J. Singleton, V. Zapf, P. Manuel, I. I. Mazin, Y. Li, H. O. Jeschke, R. Valentí, and R. Coldea, *Phys. Rev. B* **92**, 235119 (2015).
- [9] H. B. Cao, A. Banerjee, J.-Q. Yan, C. A. Bridges, M. D. Lumsden, D. G. Mandrus, D. A. Tennant, B. C. Chakoumakos, and S. E. Nagler, *Phys. Rev. B* **93**, 134423 (2016).
- [10] K. Kitagawa, T. Takayama, Y. Matsumoto, A. Kato, R. Takano, Y. Kishimoto, S. Bette, R. Dinnebier, G. Jackeli, and H. Takagi, *Nature (London)* **554**, 341 (2018).
- [11] J. G. Rau, E.-H. Lee, and H.-Y. Kee, *Phys. Rev. Lett.* **112**, 077204 (2014).
- [12] I. A. Leahy, C. A. Pocs, P. E. Siegfried, D. Graf, S.-H. Do, K.-Y. Choi, B. Normand, and M. Lee, *Phys. Rev. Lett.* **118**, 187203 (2017).
- [13] S.-H. Baek, S.-H. Do, K.-Y. Choi, Y. S. Kwon, A. U. B. Wolter, S. Nishimoto, J. van den Brink, and B. Büchner, *Phys. Rev. Lett.* **119**, 037201 (2017).
- [14] J. Zheng, K. Ran, T. Li, J. Wang, P.-S. Wang, B. Liu, Z.-X. Liu, B. Normand, J. Wen, and W. Yu, *Phys. Rev. Lett.* **119**, 227208 (2017).
- [15] A. Banerjee, P. Lampen-Kelley, J. Knolle, C. Balz, A. A. Aczel, B. Winn, Y. Liu, D. Pajerowski, J.-Q. Yan, C. A. Bridges, A. T. Savici, B. C. Chakoumakos, M. D. Lumsden, D. A. Tennant, R. Moessner, D. G. Mandrus, and S. E. Nagler, *npj Quantum Mater.* **3**, 8 (2018).
- [16] Y. Cui, J. Zheng, K. Ran, J. Wen, Z.-X. Liu, B. Liu, W. Guo, and W. Yu, *Phys. Rev. B* **96**, 205147 (2017).
- [17] S. M. Winter, Y. Li, H. O. Jeschke, and R. Valentí, *Phys. Rev. B* **93**, 214431 (2016).
- [18] A. Banerjee, J. Q. Yan, J. Knolle, C. A. Bridges, M. B. Stone, M. D. Lumsden, D. G. Mandrus, D. A. Tennant, R. Moessner, and S. E. Nagler, *Science* **356**, 1055 (2017).
- [19] K. Ran, J. Wang, W. Wang, Z.-Y. Dong, X. Ren, S. Bao, S. Li, Z. Ma, Y. Gan, Y. Zhang, J. T. Park, G. Deng, S. Danilkin, S.-L. Yu, J.-X. Li, and J. Wen, *Phys. Rev. Lett.* **118**, 107203 (2017).
- [20] W. Wang, Z.-Y. Dong, S.-L. Yu, and J.-X. Li, *Phys. Rev. B* **96**, 115103 (2017).
- [21] L. Janssen, E. C. Andrade, and M. Vojta, *Phys. Rev. B* **96**, 064430 (2017).
- [22] J. Cookmeyer and J. E. Moore, *Phys. Rev. B* **98**, 060412(R) (2018).
- [23] Z.-X. Liu and B. Normand, *Phys. Rev. Lett.* **120**, 187201 (2018).
- [24] A. Catuneanu, Y. Yamaji, G. Wachtel, Y.-B. Kim, and H.-Y. Kee, *npj Quantum Mater.* **3**, 23 (2018).
- [25] M. Gohlke, G. Wachtel, Y. Yamaji, F. Pollmann, and Y. B. Kim, *Phys. Rev. B* **97**, 075126 (2018).
- [26] I. Affleck, Z. Zou, T. Hsu, and P. W. Anderson, *Phys. Rev. B* **38**, 745 (1988).
- [27] See Supplemental Material at <http://link.aps.org/supplemental/10.1103/PhysRevLett.123.197201> for details concerning the fermionic spinon representation, IGG and PSG, finite-size effects, calculation of the dynamical structure factor, and field-induced topological states in the PKSL, which includes Ref. [28–34].
- [28] A. Kitaev, *AIP Conf. Proc.* **1134**, 22 (2009).
- [29] X.-G. Wen, *Phys. Rev. B* **85**, 085103 (2012).
- [30] H.-H. Tu, *Phys. Rev. B* **87**, 041103(R) (2013).
- [31] S. Yang, T. B. Wahl, H.-H. Tu, N. Schuch, and J. I. Cirac, *Phys. Rev. Lett.* **114**, 106803 (2015).
- [32] M. Greiter and R. Thomale, *Phys. Rev. Lett.* **102**, 207203 (2009).
- [33] Z.-X. Liu, H.-H. Tu, Y.-H. Wu, R.-Q. He, X.-J. Liu, Y. Zhou, and T.-K. Ng, *Phys. Rev. B* **97**, 195158 (2018).

- [34] C. Nayak, S. H. Simon, A. Stern, M. Freedman, and S. D. Sarma, *Rev. Mod. Phys.* **80**, 1083 (2008).
- [35] X.-G. Wen, *Phys. Rev. B* **65**, 165113 (2002).
- [36] X.-Y. Song, Y.-Z. You, and L. Balents, *Phys. Rev. Lett.* **117**, 037209 (2016).
- [37] Y.-Z. You, I. Kimchi, and A. Vishwanath, *Phys. Rev. B* **86**, 085145 (2012).
- [38] H.-C. Jiang, Z.-C. Gu, X.-L. Qi, and S. Trebst, *Phys. Rev. B* **83**, 245104 (2011).
- [39] H. J. Liao, R. Z. Huang, Y. B. Guo, Z. Y. Xie, B. Normand, and T. Xiang (unpublished).
- [40] V. Kalmeyer and R. B. Laughlin, *Phys. Rev. Lett.* **59**, 2095 (1987).
- [41] Y. Kasahara, T. Ohnishi, Y. Mizukami, O. Tanaka, S. Ma, K. Sugii, N. Kurita, H. Tanaka, J. Nasu, Y. Motome, T. Shibauchi, and Y. Matsuda, *Nature (London)* **559**, 227 (2018).